

## Electronic and superconducting properties of the $Ti_3P$ -type compounds $Nb_3As$ and $Nb_3Si$

D. U. Gubser and R. A. Hein

*U. S. Naval Research Laboratory, Washington, D. C.*

R. M. Waterstrat

*National Bureau of Standards, Washington, D. C.*

A. Junod

*Université de Genève, 1211 Genève, Switzerland*

(Received 25 March 1976)

Superconductivity has been observed below temperatures of about 0.3 K in the tetragonal  $Ti_3P$ -type compounds  $Nb_3Si$  and  $Nb_3As$ . Measurements of the electrical resistivity, heat capacity, superconducting transition temperature, and the critical magnetic field curve are reported. From these measurements, values of the electronic specific-heat coefficient  $\gamma$ , the Debye temperature  $\Theta$ , the electron-phonon coupling constant  $\lambda$ , and the Ginzburg-Landau parameter  $\kappa$ , are deduced. Both compounds have low  $\gamma$  values ( $\gamma_{Nb_3Si} \approx 2.15$  mJ/K<sup>2</sup>g-atom and  $\gamma_{Nb_3As} \approx 0.9$  mJ/K<sup>2</sup>g-atom) which probably accounts for the low transition temperatures. A comparison of their electronic and superconducting properties with those of  $A_3B$  compounds of the  $A15$  type suggests that the electron-phonon interaction is quite large in these  $Ti_3P$ -type materials.

### I. INTRODUCTION

There is considerable interest in the stoichiometric compounds  $Nb_3Si$  and  $Nb_3As$  since some empirical relationships indicate that, if these were  $A15$ -type compounds, they would have superconducting transition temperatures ( $T_0$ ) in excess of 25 K.<sup>1-3</sup> Unfortunately, the stoichiometric  $A15$  structure is not observed for either  $Nb_3Si$  or  $Nb_3As$ . Various reasons may be offered as to why the cubic  $A15$  structure does not occur for these compounds, such as atomic-size considerations; but a completely satisfactory explanation is not yet available.

$A_3B$  compounds with a tetragonal structure of the  $Ti_3P$  type exist in both the Nb-Si and Nb-As systems.<sup>4</sup> These compounds have so far received little attention experimentally. However, since it is this structure, and not the  $A15$  type that forms at the 3-to-1 ratio, it is important to investigate the structural and electronic properties of these compounds. If one could learn how to make the  $Ti_3P$  structure unstable, perhaps the  $A15$  phase would form.

In this paper we report the first observation of superconductivity in  $Ti_3P$ -type crystal structures. The binary compounds  $Nb_3Si$  and  $Nb_3As$  were found to be superconducting at temperatures below 0.3 K. We have measured some of the superconducting and electronic properties of these compounds. (Structural considerations have been discussed previously.<sup>4,5</sup>) Galasso and Pyle<sup>6</sup> measured  $Nb_3Si$  in the  $Cu_3Au$ -type crystal structure and reported it superconducting at 1.5 K; however, this compound is now believed not to be the binary  $Nb_3Si$ , but

rather a ternary alloy containing O or N.<sup>5</sup> Indeed, the binary  $Ti_3P$  phase of  $Nb_3Si$  had been previously cooled to 0.5 K with no observation of superconductivity.<sup>5</sup>

### II. SAMPLE PREPARATION

Two samples of the compound  $Nb_3Si$  were used in this study. The sample used for measurements of superconductivity and electrical resistivity was obtained from the Albany Metallurgy Research Center at the U. S. Bureau of Mines, where it had been prepared in connection with a previous study by Deardorff *et al.*<sup>7</sup> The melting and casting procedures are described in their paper. They employed arc melting and a special chill-casting method which was observed to produce less segregation, on cooling, than conventional methods. The ingot used in the present study was received in the "as-cast" condition and it was necessary to anneal it in order to form the  $Nb_3Si$  compound. A 3-g sample was heated in a high-vacuum ( $10^{-6}$  Torr) furnace at 1850 °C for 24 h. This was followed by rapid cooling which was accomplished by turning off the furnace power and directing a jet of argon gas onto the sample. A rapid quench is necessary since  $Nb_3Si$  is stable only above 1790 °C and will decompose to form a Nb solid solution containing about 1% Si and the compound  $Nb_5Si_3$ . The extent of decomposition during cooling depends on the cooling rate of the argon jet and the size of the sample.

It was necessary to use a larger sample for the specific-heat measurements; consequently, a 6.5-g sample was arc melted at the Université de

Genève using high-purity Nb and Si and annealing treatments identical to those described above. Since the larger size reduced the effectiveness of the quench, the 6.5-g sample contained about (10–20)% of the decomposition products, whereas the 3-g sample contained only (2–3)% of these phases. In both samples, however, the major constituent, as revealed by x-ray diffraction, was the compound  $\text{Nb}_3\text{Si}$  in the  $\text{Ti}_3\text{P}$ -type structure.

The sample of  $\text{Nb}_3\text{As}$  was prepared by mixing Nb and As powders in the desired proportions and compressing the mixture into a cylinder weighing about 10 g. This was placed in a BeO crucible and melted in an rf furnace under pressurized argon (40 atm) at the Université de Genève. The melt was allowed to solidify by cooling to about 1600 °C, where it was homogenized for 6 hours and then cooled by turning off the furnace power. It appeared that there was little weight loss during these procedures but losses could not be checked directly since portions of the ingot adhered to the crucible. X-ray diffraction patterns of this material indicated that it was predominantly the  $\text{Ti}_3\text{P}$ -type compound  $\text{Nb}_3\text{As}$ . This sample and the 3-g sample of  $\text{Nb}_3\text{Si}$  both contained sizable single crystals. These were used in a structure refinement which has been published elsewhere.<sup>4</sup>

### III. NORMAL-STATE PROPERTIES

#### A. Heat capacity

Specific-heat data were collected at the Université de Genève using an adiabatic calorimeter which was provided with a mechanical heat switch. Temperatures below 4.2 K were determined with a carbon-film temperature sensor, deposited on the sample, that was calibrated against <sup>4</sup>He vapor-pressure gas thermometry. Above 4.2 K a <sup>4</sup>He gas

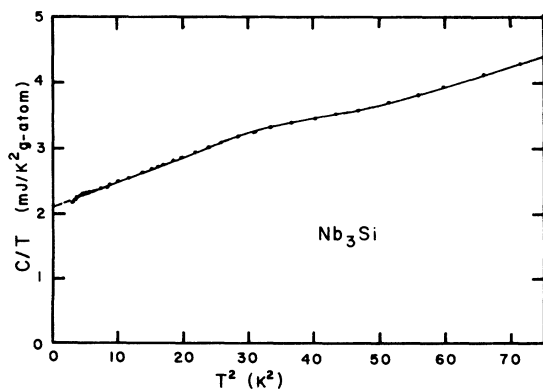


FIG. 1. Specific-heat data for the 6.5-g sample of  $\text{Nb}_3\text{Si}$ . Nonlinear effects below  $T^2$  of 50  $\text{K}^2$  ( $\sim 7$  K) are presumably due to particles of the Nb(Si) solid solution which is present in the sample (see text).

thermometer was used.

Figure 1 shows the specific-heat data obtained on the 6.5-g  $\text{Nb}_3\text{Si}$  sample. Traces of a broad band transition are found between 5.5 and 7.5 K which we attribute to small amounts of Nb-solid-solution particles in the sample (see Sec. II). Neglecting this anomaly, and giving more weight to the high-temperature part of the curve, the data fit the two-term polynomial

$$C = \gamma T + \frac{12}{5} \pi^4 R (T/\Theta)^3, \quad (1)$$

where  $\gamma$  is the linear coefficient of normal-state electronic specific heat,  $\Theta$  is the Debye temperature, and  $R$  is the universal gas constant. The values for  $\gamma$  and  $\Theta$  are

$$\begin{aligned} \gamma &= 2.15 \pm 0.15 \text{ mJ/K}^2 \text{ g-at.} \\ &= 2100 \pm 150 \text{ erg/K}^2 \text{ cm}^3 \end{aligned}$$

and

$$\Theta = 400 \pm 30 \text{ K.}$$

The estimated error limits take into account compositional uncertainties.

#### B. Resistivity

Normal-state resistivities, averaged over all crystalline directions and sample inhomogeneities, of both  $\text{Nb}_3\text{Si}$  and  $\text{Nb}_3\text{As}$  were measured at 300 and 4.2 K by an ac mutual-inductance technique.<sup>5</sup> The sample was placed within a coil system and the sample-induced change in the out-of-phase component of the mutual inductance  $\Delta\chi''$  of the coil system was recorded. When the skin depth is much greater than the radius of the sample, or alternatively, when the resistivity  $\rho$  of the sample satisfies the condition

$$\rho > 10^3 a^2 f, \quad (2)$$

where  $\rho$  is in  $\Omega \text{ cm}$ ,  $a$  is the radius in cm, and  $f$  is the frequency in Hz, the change in  $\Delta\chi''$  is proportional to the inverse of the sample's resistivity. To calibrate the coil system and to minimize size-effect errors due to irregularly shaped samples, a piece of nonmagnetic 301 stainless steel (ss), whose electrical resistivity was accurately known, was cut into the shape of the samples and used as a standard. Resistivities of the  $\text{Nb}_3\text{Si}$  and  $\text{Nb}_3\text{As}$  samples were then determined from the relation

$$\rho/\rho_{ss} = \Delta\chi''_{ss}/\Delta\chi''. \quad (3)$$

These values are listed in Table I.

The resistance ratio  $[\rho(300)/\rho(4.2)]$  of the 3-g  $\text{Nb}_3\text{Si}$  sample was 25:1, which indicates a high-quality sample with long electron mean free paths. The resistance ratio of the  $\text{Nb}_3\text{As}$  sample was only 4:1 and hence this sample has shorter mean free

TABLE I. List of measured and calculated parameters for  $\text{Nb}_3\text{Si}$  and  $\text{Nb}_3\text{As}$ . The number in curly brackets for the Debye temperature of  $\text{Nb}_3\text{As}$  is merely an estimate based on the measured value for  $\text{Nb}_3\text{Si}$  and the observed systematics of  $\Theta$  in  $A_{15} A_3B$  materials.

	$\text{Nb}_3\text{Si}$	$\text{Nb}_3\text{As}$	Units
$\rho(300)$	195	215	$\mu\Omega \text{ cm}$
$\rho(4.2)$	8	53	$\mu\Omega \text{ cm}$
$\rho(300)/\rho(4.2)$	25	4	
$T_0$	0.29	$\sim 0.31$	K
$(\partial H_{c2}/\partial T)_{T_0}$	$\sim 500$	$\sim 2060$	Oe/K
$\gamma$	$2.15 \pm 0.15$	$\sim 0.9$	$\text{mJ/K}^2 \text{ g-at.}$
$\gamma$	$2100 \pm 150$	$\sim 860$	$\text{erg/K}^2 \text{ cm}^3$
$\kappa$	1.8	$\sim 12$	
$\lambda$	0.37	$\sim 0.37$	
$\Theta$	$400 \pm 30$	{400}	K
$V_{\text{at}}$	10.2	10.4	$\text{cm}^3/\text{g-at.}$

paths. Since various types of lattice defects may scatter electrons and reduce the mean free path, these resistance measurements suggest that the  $\text{Nb}_3\text{Si}$  had relatively fewer defects than the  $\text{Nb}_3\text{As}$ .

#### IV. SUPERCONDUCTING PROPERTIES

Temperatures below 1 K were produced by magnetic cooling techniques employing chromium potassium alum as the working substance. Temperatures were determined from the magnetic susceptibility of chromium potassium alum (calibrated against  $^4\text{He}$  vapor pressure) and thermal contact to the samples was accomplished by embedding the samples in a bundle of copper wires which was attached to the chromium potassium alum.

The zero-magnetic-field transition temperature  $T_0$  of these samples was measured with a low-

frequency (330 Hz) ac mutual-inductance bridge. Figures 2(a) and 2(b) show the in-phase component of the susceptibility  $\chi'$  of the samples as a function of temperature.  $T_0$  is defined as the midpoint of these transitions and the values are listed in Table I. The transition width for the 3-g  $\text{Nb}_3\text{Si}$  sample was approximately 0.03 K or  $0.1T_0$ . Similar values of  $T_0$  and transition widths were obtained using portions of the 6.5-g sample. This suggests that the compound  $\text{Nb}_3\text{Si}$  possesses a rather small composition range, in agreement with the previous conclusions of Deardorff *et al.*<sup>7</sup> The observed differences in the microstructures of these two samples (see Sec. II) apparently have little effect on the measured value of  $T_0$ . The transition width of the cast and annealed  $\text{Nb}_3\text{As}$  sample, by comparison, was almost 0.2 K, beginning around 0.14 K and ending near 0.34 K. This suggests that larger composition variations may occur in  $\text{Nb}_3\text{As}$ . To minimize the compositional effects, very small chips of  $\text{Nb}_3\text{As}$  were taken from the central portion of this sample. These chips had much smaller transition widths [see Fig. 2(b)] than the bulk specimen although they were still appreciably larger than the  $\text{Nb}_3\text{Si}$  sample. Superconducting measurements reported are from these small central pieces of the  $\text{Nb}_3\text{As}$  ingot.

Critical magnetic fields  $H_{c2}$  of  $\text{Nb}_3\text{Si}$  and  $\text{Nb}_3\text{As}$  were measured inductively while slowly sweeping the magnetic field. The in-phase components  $\chi'$  of the susceptibility as a function of applied field are shown in Figs. 3(a) and 3(b).

Critical-magnetic-field transitions for the 3-g  $\text{Nb}_3\text{Si}$  sample were comparatively sharp; however, a distinct change in slope appeared in the transition which suggests that very small composition variations may be present in the sample. Critical magnetic fields for  $\text{Nb}_3\text{Si}$  have been defined in two

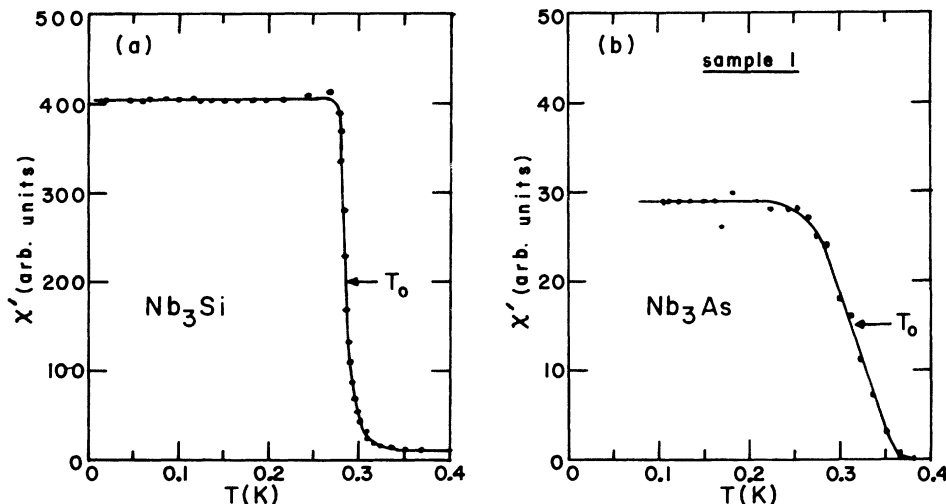


FIG. 2. Zero-magnetic-field superconducting transition temperature for  $\text{Nb}_3\text{Si}$  (a) and  $\text{Nb}_3\text{As}$  (b).  $T_0$  is defined as the midpoint of the susceptibility change.

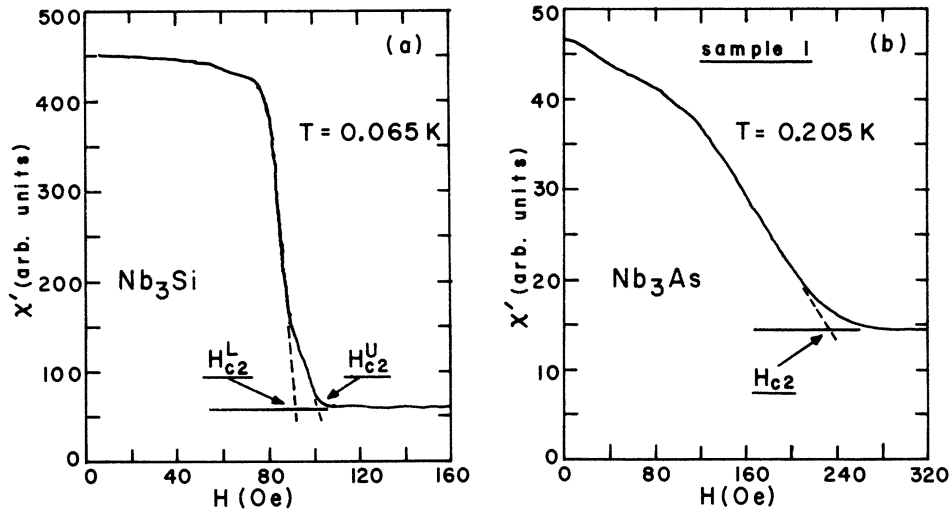


FIG. 3. Magnetic-field-induced superconducting-to-normal-state transitions for  $\text{Nb}_3\text{Si}$  (a) and  $\text{Nb}_3\text{As}$  (b). The critical magnetic fields  $H_{c2}$  are defined as shown (see text).

ways, as shown in Fig. 3(a), one being an extrapolation of the dominant susceptibility change to the normal-state axis  $H_{c2}^L$  and the other being the extrapolation of the tail portion of the susceptibility transition to the normal-state axis  $H_{c2}^U$ . The temperature dependences of these critical magnetic fields are shown in Fig. 4(a). The extrapolated zero-field transition temperatures of the two critical-magnetic-field plots show a difference of only 0.004 K; hence, if the speculation is correct that composition variations produce the noted structure in the magnetic field transitions, then the variations are very small or have little effect on  $T_0$ .

Critical-magnetic-field transitions for the  $\text{Nb}_3\text{As}$  samples were extremely broad, showing susceptibility changes immediately upon application of an applied field and then continuously changing until all the sample was driven into the normal state. The critical magnetic fields for these samples

were defined as shown in Fig. 3(b). The temperature dependences of the critical magnetic fields for two different small pieces of  $\text{Nb}_3\text{As}$  are shown in Fig. 4(b). Note that the critical magnetic fields are much larger in  $\text{Nb}_3\text{As}$  than in  $\text{Nb}_3\text{Si}$ , as would be expected in a less-pure superconductor.

#### V. CALCULATED PARAMETERS

Using the isotropic weak-coupling BCS relations<sup>9</sup>

$$\left(\frac{T_0}{H_c(0)}\right)\left(\frac{dH(T)}{dT}\right)_{T_0} = -1.737 \quad (4)$$

and

$$2\pi\gamma[T_0/H_c(0)]^2 = 1.057, \quad (5)$$

where  $H_c(T)$  is the thermodynamic critical magnetic field, one obtains

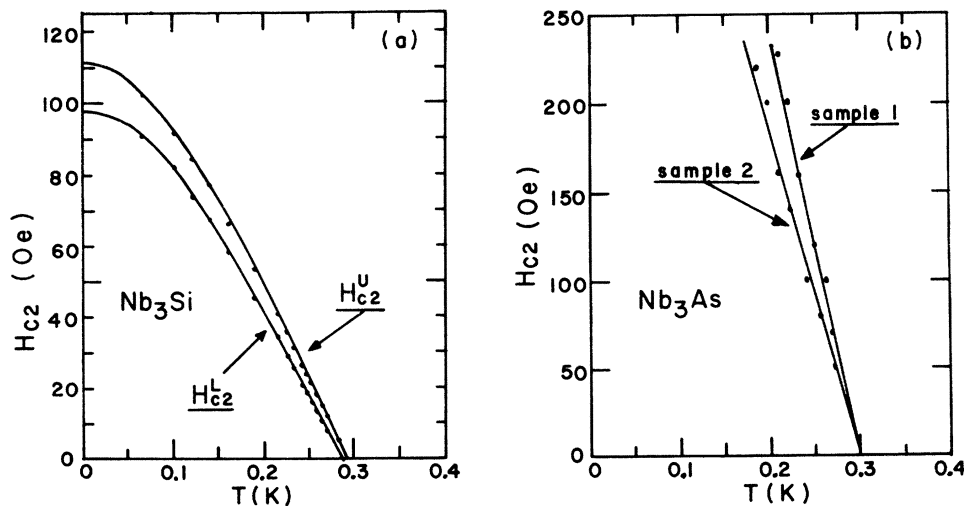


FIG. 4. Critical-magnetic-field curves for the  $\text{Nb}_3\text{Si}$  sample (a) and the  $\text{Nb}_3\text{As}$  samples (b).

$$\left(\frac{dH_c}{dT}\right)_{T_0} = 4.23\gamma^{1/2}. \quad (6)$$

Combining Eq. (6) with the Abrikosov<sup>10</sup> relation for  $H_{c2}$ ,

$$H_{c2} = \sqrt{2}\kappa H_c, \quad (7)$$

where  $\kappa$  is the Ginzburg-Landau parameter, one arrives at the expression

$$\left(\frac{dH_{c2}}{dT}\right)_{T_0} \approx 6\kappa\gamma^{1/2}. \quad (8)$$

For  $\text{Nb}_3\text{Si}$ ,  $\gamma$  and  $(dH_{c2}/dT)_{T_0}$  were measured (see Table I) and a  $\kappa$  value of 1.8 was determined from Eq. (8).

For  $\text{Nb}_3\text{As}$ , the specific heat was not measured; hence,  $\gamma$  as well as  $\kappa$  were unknowns. In order to estimate these values for  $\text{Nb}_3\text{As}$ , Eq. (8) is combined with the Gorkov-Goodman formula<sup>11</sup>

$$\kappa = 7.5 \times 10^3 \gamma^{1/2} \rho, \quad (9)$$

which is good in the dirty limit ( $\kappa > 10$ ) such that impurity scattering has eliminated the effects of crystalline and Fermi-surface anisotropies.<sup>12</sup> The resulting formula is

$$\left(\frac{dH_{c2}}{dT}\right)_{T_0} \approx 4.5 \times 10^4 \gamma \rho. \quad (10)$$

Because of the sample inhomogeneities, and the fact that  $\rho$  represents an average measurement for the bulk of the sample and not the small chips which were used to measure  $(dH_{c2}/dT)_{T_0}$ , only a crude estimate of  $\gamma$  can be obtained. The  $(dH_{c2}/dT)_{T_0}$  values obtained from the data shown in Fig. 4(b) are 2270 Oe/K for sample 1 and 1850 Oe/K for sample 2. These values probably reflect variations in the resistivity of the specimens since both had identical transition temperatures. Since the resistivity measured represents an average value, we chose the average  $(dH_{c2}/dT)_{T_0}$  of these two samples to calculate  $\gamma$ . The result is

$$\gamma = 860 \pm 100 \text{ erg/cm}^3 \text{K}^2,$$

and from Eq. (9),

$$\kappa \approx 12,$$

which is within the dirty limit, where one would expect Eq. (9) to hold.

The electron-phonon coupling constant for  $\text{Nb}_3\text{Si}$  can be calculated from the McMillan equation

$$T_0 = \frac{\Theta}{1.45} \exp \left[ - \left( \frac{1.04(1+\lambda)}{\lambda - \mu^*(1+.62\lambda)} \right) \right], \quad (11)$$

where  $\Theta$  is the Debye temperature and  $\mu^*$  is the Coulomb repulsion term, which we take to be 0.13. From the heat-capacity measurements,  $\Theta_{\text{Nb}_3\text{Si}}$  was determined to be 400 K; hence,

$$\lambda_{\text{Nb}_3\text{Si}} \approx 0.37.$$

The electron-phonon coupling constant cannot be calculated for  $\text{Nb}_3\text{As}$  since the value of  $\Theta_{\text{Nb}_3\text{As}}$  is not known; however, based on the observations of  $A_{15}$ ,  $A_3B$  compounds, it is estimated that  $\Theta_{\text{Nb}_3\text{Si}} \approx \Theta_{\text{Nb}_3\text{As}}$  and consequently  $\lambda_{\text{Nb}_3\text{Si}} \approx \lambda_{\text{Nb}_3\text{As}}$ .

## VI. DISCUSSION

There is considerable justification for regarding the compounds  $\text{Nb}_3\text{Ge}$  and  $\text{Nb}_3\text{Si}$  as being "isoelectronic" in view of the similar electronic structures of Ge and Si, and their location in the Periodic Table. It is, therefore, surprising that  $\text{Nb}_3\text{Ge}$  possesses a cubic  $A_{15}$ -type structure ( $T_0 \sim 23$  K) whereas  $\text{Nb}_3\text{Si}$  possesses a tetragonal  $\text{Ti}_3\text{P}$ -type structure ( $T_0 \sim 0.3$  K). The different crystal structures of these two compounds can be attributed to "atomic-size" considerations since Si atoms are smaller than Ge atoms, but this would not explain the occurrence of the same tetragonal structure in the  $\text{Nb}_3\text{As}$  compound, since Ge atoms and As atoms have nearly identical sizes. There are some reasons for attributing the stability of the  $\text{Ti}_3\text{P}$ -type structures to the existence of strong electrochemical interactions between the transition elements and nontransition elements which comprise these compounds.<sup>4,5</sup> This may be responsible for the existence of localized "partially covalent" bonding characteristics, although the overall nature of the bonding is predominantly metallic.

The high- $T_0$   $A_{15}$ -type ( $A_{3-x}B_{1+x}$ ) compounds are characterized structurally by orthogonal linear chains of  $A$  atoms and show evidence of structural instability, which is manifested by the presence of unusually "soft" phonon modes. The greatest instability in the  $A_{15}$  compounds seems to occur at or near "ideal" stoichiometry ( $A_3B$ ), where the presence of maximum long-range atomic ordering is often responsible for relatively high  $T_0$  values. For example, the  $A_{15}$  compound  $\text{Nb}_3\text{Ge}$  is not stable at "ideal" stoichiometry but the  $A_{15}$  structure ( $\text{Nb}_{2.2}\text{Ge}_{1.8}$ ) is stable, presumably due to the excess of Nb atoms. The  $A_{15}$  structure may also be stabilized at "ideal" stoichiometry by atomic defects which are introduced during vapor quenching.

The  $\text{Ti}_3\text{P}$  compounds, on the other hand, do not have a structure composed of orthogonal linear chains and they do not exhibit structural instabilities at the "ideal" stoichiometry. It appears that strong electrochemical interactions may exert a stabilizing influence on the  $\text{Ti}_3\text{P}$ -type structure and have a destabilizing effect on the  $A_{15}$ -type structure. It is, therefore, of considerable theoretical

and practical interest to deduce how such interactions would affect the structure of these compounds.

The low values of  $T_0$  in these  $Ti_3P$  compounds are understandable in light of their low- $\gamma$  values. Approximately 10–15 A15 compounds are known to have  $\gamma$  values in the range of  $Nb_3Si$  ( $2 < \gamma < 3$  mJ/K<sup>2</sup> g-atom).<sup>13</sup> Of these compounds, roughly half are not superconductors, while the others become superconducting only below 2 K. The  $\gamma$  value of  $Nb_3As$ , on the other hand, is so low that it is surprising

that it is a superconductor at all — yet it has a  $T_0$  that is slightly higher than that of  $Nb_3Si$ . No reference to any A15 compound with a  $\gamma$  value as low as that of  $Nb_3As$  (0.9 mJ/K<sup>2</sup> g-atom) has been found. The electron-phonon interaction in  $Nb_3As$  and  $Nb_3Si$  must be quite strong for them to be superconductors at all. It is, therefore, of considerable theoretical interest to understand how these electrochemical interactions, which seem to stabilize the  $Ti_3P$  crystal structure, affect the superconducting behavior of these compounds.

<sup>1</sup>L. Gold, *Phys. Status Solidi* **4**, 261 (1964).

<sup>2</sup>D. Dew-Hughes and V. G. Rivlin, *Nature* **250**, 435 (1975).

<sup>3</sup>D. Dew-Hughes, *Cryogenics* **15**, 435 (1975).

<sup>4</sup>R. M. Waterstrat, K. Yvon, H. D. Flack, and E. Parthé, *Acta Crystallogr. B* **31**, 2765 (1975).

<sup>5</sup>R. M. Waterstrat, *J. Less-Common Met.* **43**, 105 (1975).

<sup>6</sup>F. Galasso and J. Pyle, *Acta Crystallogr.* **16**, 228 (1963).

<sup>7</sup>D. K. Deardorff, R. E. Siemens, P. A. Romans, and R. A. McCune, *J. Less-Common Met.* **18**, 11 (1969).

<sup>8</sup>R. G. Chambers and J. G. Park, *Brit. J. Appl. Phys.* **12**, 507 (1961).

<sup>9</sup>J. Bardeen, L. N. Cooper, and J. R. Schrieffer, *Phys. Rev.* **108**, 1175 (1957); D. U. Gubser, *Phys. Rev. B* **6**, 827 (1972).

<sup>10</sup>A. A. Abrikosov, *Zh. Eksp. Teor. Fiz.* **32**, 1442 (1957) [*Sov. Phys.-JETP* **5**, 1174 (1957)].

<sup>11</sup>B. B. Goodman, *IBM J. Res. Dev.* **6**, 63 (1962).

<sup>12</sup>D. E. Farrell and B. S. Chandrasekhar, *Phys. Rev.* **177**, 694 (1969).

<sup>13</sup>P. Spitzli, thèse No. 1541 (l'Université de Genève, Genève, Switzerland, 1970) (unpublished).